Small ORF16 modulates the Mtr complex activity in *Methanosarcina mazei* Gö1 depending on the molecular hydrogen availability

Tim Habenicht[a]; Bjarne Hastedt[a], Liam Cassidy[c], Claudia Kießling[a], Andreas Tholey[c], Jan M. Schuller[b], and Ruth A. Schmitz[a#]

[a] Institute for General Microbiology, Kiel University, 24118 Kiel, Germany

[b] SYNMIKRO Research Center and Department of Chemistry Philipps University Marburg, Karl-von-Frisch-Straße 14, 35043 Marburg

[c]Systematic Proteome Research & Bioanalytics, Institute for Experimental Medicine, Kiel University, 24105 Kiel, Germany

Adress correspondence to: Ruth A. Schmitz, e-mail: rschmitz@ifam.uni-kiel.de

Abstract Number of words: 215

Small open reading frame (small ORF)-encoded proteins, with less than 100 amino acids in length, have attracted increasing attention over the past decade after being largely overlooked due to limitations in classical bioinformatics and biochemical methodologies. For the mesophilic archaeal model system *Methanosarcina mazei* Gö1, a high number of previously unannotated small ORFs have been identified through ribosome profiling combined with LC-MS/MS analysis. However, the physiological role of the majority of the respective small proteins remains unknown. Here, we report on the functional characterization of the small ORF16 encoded small protein MtrR (49 amino acids). We demonstrate that MtrR is forming oligomers localized at the cytoplasmic membrane. There, it interacts with the tetrahydrosarcinapterin S-methyltransferase (Mtr), a key membrane-bound complex of the energy metabolism, and impacts its activity. In vitro interaction and in vivo copurification assays showed MtrR interaction with the Mtr-complex, which was further validated by microscale thermophoresis analysis demonstrating a specific strong interaction with the MtrA subunit. Analyzing growth under varying molecular hydrogen (H_2) availability demonstrated that the small ORF16 deletion mutant showed significantly impaired growth in the presence of H_2, independent of the carbon source. Consequently, we propose that MtrR fine-tunes the activity of the Mtr-complex in response to fluctuating H_2 availabilities, allowing to adapt the energy metabolism to changing environmental H_2 conditions.

Introduction

Small proteins in prokaryotes with a size of less than 100 amino acids (aa) play important roles in diverse cellular processes such as metabolism, stress response or regulation of transcription and translation (Gray et al., 2022; Jordan et al., 2023; Storz et al., 2014; Weidenbach et al., 2021). However, they have been overlooked for a long time due to technical limitations e.g. in biochemical detections. Consequently, the small proteome of most microorganisms is still relatively understudied, in particular the small proteome of archaea. Only recently, catalogs of small proteins have been identified by systematic genome-wide identification methods like ribosome footprinting (Ribo-Seq) and liquid chromatography-coupled tandem mass spectrometry (LC-MS/MS). But still, for the majority of these newly identified small proteins, functional analyses are either scarce or entirely lacking (Gelsinger et al., 2021; Gray et al., 2022; Hadjeras et al., 2023; Jordan et al., 2023; Storz et al., 2014; Weidenbach et al., 2021).

In archaea, recent global studies employing mass spectrometry and Ribo-Seq analysis to identify new small proteins encoded by small ORFs have been reported for *Haloferax volcanii* (Hadjeras et al., 2023) and *Methanosarcina mazei* Gö1 (Tufail et al., 2024). For *H. volcanii*, 48 novel small ORFs have been identified, including HVO_2753 and HVO_0758 (Hadjeras et al., 2023; Üresin et al., 2023). Those encode small zinc finger proteins (59 and 56 aa, respectively) that influence swarming activity and biofilm formation (Üresin et al., 2023; Zahn et al., 2021). In the methanoarchaeal model system *M. mazei*, preceding LC-MS/MS analysis has identified 69 small proteins (Cassidy et al., 2021; Prasse et al., 2015; Weidenbach et al., 2021). Only a few of those have been functionally characterized. Examples are the small protein sP36 (61 aa), which is responsible for the regulation of an ammonium transporter $AmtB_1$ (Habenicht et al., 2023) and the small protein sP26 (23 aa) impacting activity of the glutamine synthetase $GlnA_1$ (Gutt et al., 2021). The recent global Ribo-Seq analysis combined with LC-MS/MS identified 314 previously unannotated small ORFs. Among these, several were highly regulated in response to nitrogen availability (Tufail et al., 2024). This comprehensive analysis uncovering a pleiotropy of novel small ORFs now opens up a new avenue to start elucidating the functions of small proteins in *M. mazei*.

Methanoarchaea are predominantly responsible for the global biotic production of the green-house gas methane. Methane is produced under anoxic conditions through one of three main pathways: acetoclastic, methylotrophic, and hydrogenotrophic methanogenesis (Costa & Leigh, 2014). During acetoclastic methanogenesis, acetate is converted to methane and carbon dioxide, where the cleavage step of the C-C bound is catalyzed by the key enzyme, the Acetyl-CoA decarbonylase/synthase complex (ACDS) (Grahame, 1991). The hydrogenotrophic pathway reduces carbon dioxide to methane by using molecular hydrogen (H_2), which serves as electron donor. The

methylotrophic pathway uses methylated compounds such as methanol, methylamines ore methyl sulfides (Costa & Leigh, 2014; Uwe Deppenmeier et al., 1996; Hippe et al., 1979; Huang et al., 2020; Mand & Metcalf, 2019). All pathways share, the methane formation from methyl-coenzyme-M as well as the heterosulfide reductase (Hdr) which reduces the CoM-S-S-CoB heterodisulfate and regenerates CoM and CoB (Hedderich et al., 2005; Jaun & Thauer, 2007).

The genus *Methanosarcina* has the unique ability to use all three main pathways for methanogenesis (Hippe et al., 1979; Mand & Metcalf, 2019). This way, *Methanosarcina* species show a high level of adaptability regarding available carbon and energy sources, in contrast to otherwise rather specialized methanoarchaea like *Methanobrevibacter* and *Methanococcus* (both mainly hydrogenotrophic), *Methanosphaera* (methylotrophic) and *Methanosaeta* (acetoclastic) (Liu & Whitman, 2008). Naturally, in *Methanosarcina*, these pathways are regulated depending on the environmental conditions, whereby the energy output differs depending on the substrates (Liu & Whitman, 2008). Methanogenesis using H_2 in combination with CO_2 (-136 kJ/mol CH_4) or growth on methylated substrates (-108 kJ/mol CH_4) is far more exergonic compared to acetoclastic methanogenesis (-65 kJ/mol CH_4) (Yi et al., 2023).

In the presence of H_2, *M. mazei* grows hydrogenotrophic, reducing CO_2 to methane (C_1-metabolic pathway). The stepwise reduction of CO_2 bound to cofactors is initiated with the reduction of CO_2 to a formyl group bound to the cofactor methanofuran (MFR). This formyl group is then transferred to the second cofactor tetrahydrosarcinapterin (H_4SPT), and further reduced generating methenyl-H_4SPT. Subsequent reduction yield methyl-H_4SPT, of which the methyl group is then transferred to the third cofactor, coenzyme M (CoM), by the membrane-bound tetrahydrosarcinapterin S-methyl transferase (Mtr)-complex. In the final step of methanogenesis, the methyl group is reduced to methane by the methyl-CoM reductase. Electrons required for all reduction steps are supplied by H_2 oxidation. In the absence of sufficient H_2, *M. mazei* can also use methylated compounds as a carbon and energy source (methylotrophic growth). However, without the external electron donor H_2, reducing equivalents must come from an alternative source. To achieve this, a fraction of the methyl groups is oxidized to CO_2, providing the electrons for the reduction of further methyl groups to methane. This disproportionation process involves reversing part of the C_1 metabolic pathway, where enzymes that normally reduce the C_1 compounds now proceed in the reverse direction and oxidize methyl groups to CO_2. The first step in this process is the transfer of the methyl group from methyl-CoM to H_4SPT, catalyzed by the Mtr-complex running in reverse direction (Uwe Deppenmeier et al., 1996).

Until today, substrate-dependent regulation of metabolic pathways in response to different available carbon and energy sources has been shown for *Methanosarcina* species mainly on transcriptional

level. For example, in *M. acetivorans*, the expression of methyltransferase MtaC1 and MtaB1, which transfer the methyl group of methanol to CoM, are upregulated when methanol is present. However, in the presence of acetate as sole carbon and energy source, the expression of the ACDS complex is upregulated (Li et al., 2007). Still, the molecular mechanisms of those regulatory processes on the transcriptional level are often not entirely understood; besides, post-transcriptional and post-translational regulation has not been reported yet. In addition to the carbon and energy source, highly energy dependent anabolic processes might also impact or regulate the energy pathways like e.g. the nitrogen source and availability (Yi et al., 2023).

In this report, we aimed to study the physiological role of the 49-aa protein encoded by small ORF16 in *M. mazei*, which has been shown to be significantly transcribed and translated (Tufail et al. 2024). We show experimental evidence that the respective small protein, which was termed MtrR, is localized exclusively at the cytoplasmic membrane, despite lacking any transmembrane domains. This membrane association is based on the interaction with the subunit A of the membrane-bound Mtr complex (MtrA). Based on our findings from biochemical and genetic approaches to characterize this small protein, we propose that MtrR is responsible for fine tuning the Mtr complex in response to the availability of H_2 by impeding the methyl transfer from CoM to H_4SPT most likely through direct protein-protein interaction.

Results

Cellular localization of oligomeric MtrR at the cytoplasmic membrane

We aim to investigate the physiological role of the small ORF16 encoded small protein in *M. mazei*, from here on referred to as MtrR, which was identified by Ribo-Seq analysis and verified on protein level by LC-MS/MS (Tufail et al., 2024).

MtrR was fused to a C-terminal his-tag (MtrR-His_6), heterologously expressed in *Escherichia coli* and purified by Ni-NTA immobilized metal affinity chromatography (IMAC). The obtained elution fractions at low imidazole concentration showed, in addition to a dimeric MtrR-His_6 (approx. 14 kDa), distinct proteins of higher apparent molecular weight, potentially representing higher oligomers, which were not present in following elutions with higher imidazole concentrations (Fig. 1A). Subsequent size exclusion chromatography (SEC) using an Enrich 70 column (BioRad, Hercules, USA) yielded a fraction of MtrR-His_6 purified to apparent homogeneity (Fig. 1B). Because the aa-sequence of MtrR does not contain any tryptophan, tyrosine or cysteine residues, the SEC shows no visible peaks in the UV_{280nm} chromatogram. Consequently, an exact determination of the molecular weight is difficult. Calibration with standard proteins showed that the smallest MtrR-His_6 fraction (13 ml elution volume)

corresponds to a molecular mass of approximately 10 kDa, representing dimeric MtrR-His_6 (supplemental Fig. S1). In the preceding elution fractions (11 and 12 ml), additional higher oligomers of MtrR were detected (Fig. 1B). Therefore, we propose that in isolation MtrR forms dimers and higher oligomeric forms.

To analyze the cellular localization and potential oligomerization of MtrR in its native background, tagged versions of MtrR were expressed in *M. mazei* from plasmids and subcellular fractions were subjected to western blot analysis. For this purpose, the gene encoding MtrR-His_6 was cloned under the control of the constitutive promoter PmcrB (pRS2087, MtrR-His_6). In a second construct, small ORF16 under its native promoter was fused to an N-terminal spa-tag (pRS1639, spa-MtrR). After harvesting *M. mazei* cells carrying either pRS2087 or pRS1639 during exponential growth, cytoplasmic and membrane fractions were generated by ultracentrifugation of cell lysates. Both fractions were analyzed by western blot using antibodies directed against the respective tags. Regardless of the protein tag or promoter used, MtrR was exclusively detected in the membrane fraction and not in the cytoplasmic fraction (Fig. 1C). For both tagged versions, the western blot signals corresponded to protein masses of approximately 20 kDa, 25 kDa and 55 kDa, which might represent stable homo-oligomeric forms of MtrR, and a degradation product in case of the 20 kDa protein band. Since MtrR is a hydrophilic, rather uncharged small protein and does not contain a transmembrane domain, the in vivo membrane localization of MtrR most likely results from an interaction with membrane-associated proteins.

To further validate the oligomerization of MtrR expressed in *M. mazei* from a plasmid (pRS2087), MtrR-His_6 was purified by IMAC from the solubilized membrane fraction (2 % DDM) of exponentially growing cells. The elution fractions were analyzed by western blotting using specific antibodies generated against MtrR, which clearly demonstrated the presence of MtrR in several SDS stable higher oligomeric forms (approx. 130 kDa, 80 kDa and 60 kDa) in addition to the dimeric MtrR (14 kDa, Fig. 1D) in the native background.

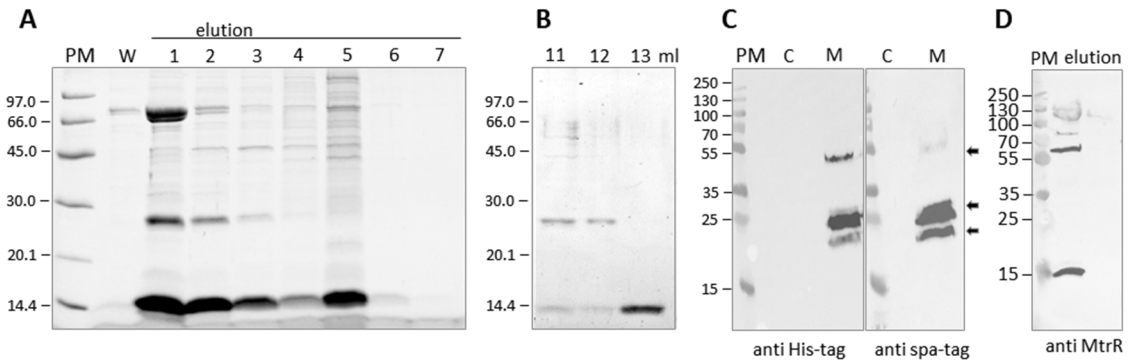

Fig. 1: Purification and cellular localization of MtrR. A: SDS PAGE of IMAC purification of heterologously expressed MtrR-His_6. W: Last wash fraction; lanes 1-4: 100 mM imidazole; lanes 5-7, 250 mM imidazole. **B:** SEC purification of MtrR-His_6 (Enrich SEC 70 column; BioRad, Hercules, USA) for downstream applications (pull down experiments and antibody generation); a protein mix (BioRad size-exclusion standard) was used as a standard for calibration, depicted are the fractions 11-13 ml. The elution fraction at 13 ml corresponds to a molecular mass of approximately 10 kDa (see supplemental Fig. S1). **C:** Exponential growing *M. mazei* cells expressing MtrR-His_6 or spa-MtrR from a plasmid (pRS2087 and pRS1693, respectively) were harvested, fractionated, and subcellular fractions analyzed by western blot using antibodies targeting either His-tag or strep-tag. MtrR presence in the membrane fraction is depicted by arrows, corresponding to protein (complexes) with a molecular mass of approximately 20 kDa, 25 kDa and 50 kDa. C, cytoplasmic fraction; M, membrane fraction. The SDS-PAGE was loaded with 0.4 mg protein of both subcellular fractions. PM, PageRuler Plus Prestained Protein Ladder (Thermo Fisher Scientific, Waltham, MA, USA). **D:** In vivo copurification: MtrR-His_6 was constitutively expressed in *M. mazei* (pRS2087) and purified from the solubilized membrane fraction (2 % DDM) by IMAC. Elution fraction 2 of the purified MtrR complex was analyzed by western blot using antibodies generated against MtrR. Arrows indicate MtrR detected in complexes with a higher molecular mass (60 kDa, 80 kDa and 130 kDa).

The small protein MtrR interacts with the tetrahydrosarcinapterin S-methyl transferase (Mtr) complex

The localization at the membrane prompted us to identify target proteins of the small protein MtrR in the membrane fraction using purified recombinant MtrR-His_6 as bait-protein for in vitro pull-downs of potentially interacting proteins from solubilized membrane fractions. Membrane fractions of *M. mazei* were prepared from exponentially growing cells by ultracentrifugation and solubilization with 2% DDM. 0.5 mg purified MtrR-His_6 was incubated with 5 mg of membrane fraction proteins for 30 min followed by IMAC purification of MtrR-His_6. In three independent biological replicates, two protein signals, at a size of 25 kDa and 35 kDa, were repeatedly detected to co-purify with MtrR-His_6 as shown by denaturing SDS-PAGE (Fig. 2 A). These additional bands were not detected when using only the membrane fraction in the absence of the bait MtrR-His_6 as a negative control (supplemental Fig. S2). The proteins were identified by mass spectrometry with high confidence as tetrahydrosarcinapterin S-methyl transferase (Mtr) subunit A and subunit H in three independent biological replicates including controls (supplemental Fig. S2). MtrA and MtrH are two subunits of the large trimeric Mtr-complex ($MtrABCDEFGH_2$), which represents a membrane-bound key protein complex of the energy metabolism, transferring the methyl group from methyl- H_4SPT to the next cofactor, CoM. Out of the eight different subunits, MtrH and MtrA are the two most hydrophilic subunits of Mtr, with MtrH being completely soluble and forming dimers which are linked to the membrane only by interaction with the subunits MtrB and MtrF (Reiff-Trautmannsdorf et al. *in preparation*). MtrA contains a large cytoplasmic domain and a small transmembrane helix anchoring

it tightly to the stem of the trimeric Mtr complex. Due to this interaction with the Mtr complex, the small protein encoded by small ORF16 was termed MtrR.

To verify the interaction with the Mtr complex, a reverse approach was tested by an in vivo copurification using strep-MtrE constitutively expressed from a plasmid (pRS1743) in *M. mazei* to purify the Mtr complex and potential interaction partners such as MtrR from solubilized cell extract (1% LMNG, Reiff-Trautmannsdorf et al. *in preparation*). The elution fraction of the purified strep-tagged MtrE analyzed on SDS PAGE showed the correct protein pattern as reported by Reiff-Trautmannsdorf et al. *in preparation*, including the 28 and 35-kDa subunits MtrA and MtrH (Fig. 2B). The elution fraction was further analyzed by western blot, using antibodies against strep-tag and MtrR. Using the strep-tag antibodies, MtrE was mainly detected as monomer (30 kDa), but was also detected in several complexes with molecular masses of 50 kDa, 60 kDa and 70 kDa, which might correspond to complexes with different interacting Mtr subunits (Fig. 2C, left panel). When using specific antibodies, MtrR was clearly detected in the purified Mtr-complex (Fig. 2C, mid panel) in contrast to the respective control (Fig. 2C, right panel). MtrR was present as a dimer (approx. 14 kDa) as well as in complexes of 30 kDa, 60 kDa and 130 kDa. Notably, this complex MtrR pattern closely mirrors the one observed in the MtrR-His_6 purification (Fig. 1D), demonstrating a consistent oligomerization pattern of MtrR in *M. mazei*. Consequently, this coelution confirms that MtrR copurifies with the Mtr complex, as also demonstrated by the pull-down (Fig. 2A), and further points towards higher MtrR oligomers in the Mtr complex.

The soluble domain of the MtrA subunit (M1 – S168) without the hydrophobic membrane anchor (E169 - R240) was cloned as a strep-tagged version in *E. coli* and purified by affinity chromatography. Interaction analysis with purified, fluorescently labeled MtrA (MtrA-RED, 20 nM) was performed by microscale thermophoresis (MST) using unlabeled MtrR ranging from 3 nM to 100 µM. The affinity analysis using MO.Affinity (Nanotemper, Munich, Germany) resulted in an estimated dissociation constant of K_D = 110 ± 30 nM. In two independent biological replicates, MST analysis showed a strong interaction between MtrA-RED and MtrR in vitro, supporting our in vitro pull-down and in vivo copurification experiments.

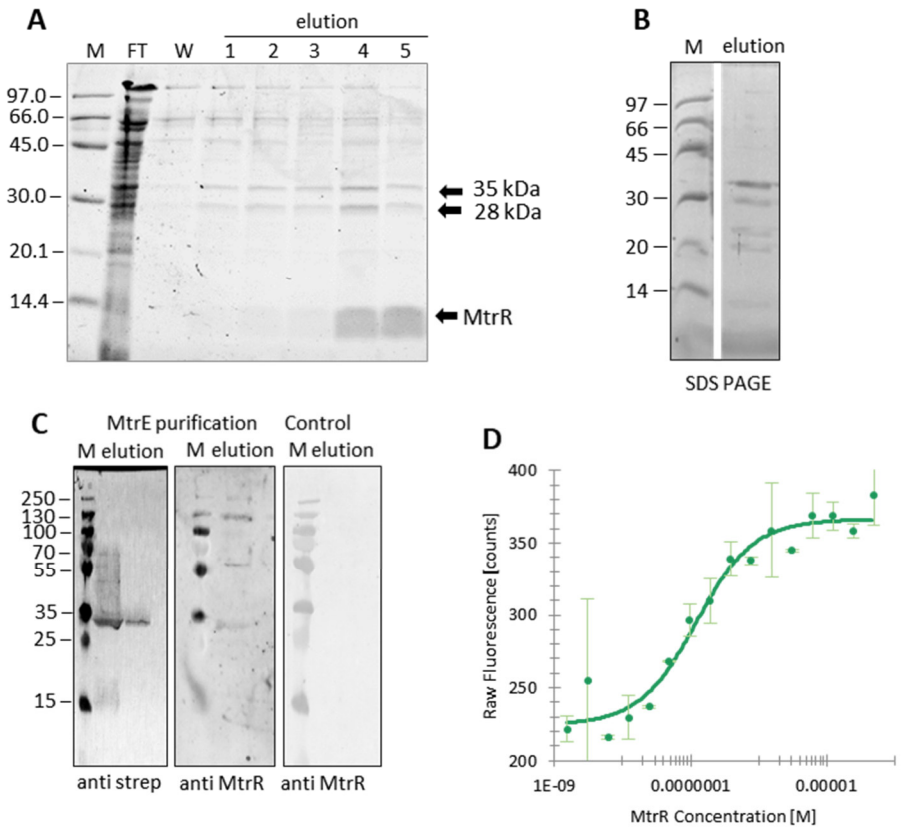

Fig. 2: MtrR binds Mtr-complex in particular MtrA. A: Pull-down analysis using purified MtrR-His$_6$ as bait against solubilized *M. mazei* membrane fractions (2 % DDM). After 30 min incubation at RT, MtrR-His$_6$ was purified by IMAC revealing two additional distinct protein bands as indicated. **B and C: In vivo co-purification of the Mtr complex from *M. mazei* using plasmid encoded strep-MtrE**. **B**: Elutions of the strep-tactin purified complex were analyzed by SDS PAGE. Visible are the different copurified subunits of the Mtr complex **C:** Elutions of the strep-tactin purified complex were analyzed by western blot using antibodies directed against the strep-tag or specifically against MtrR, demonstrating coelution of MtrR with the Mtr complex purified by strep-MtrE at approximately 30 kDa, 60 kDa and 130 kDa. *M. mazei* WT cells not encoding any strep tagged proteins were used as control (right panel). **D: Affinity analysis of the MtrR-MtrA interaction by Microscale thermophoresis.** 20 nM RED labeled heterologously expressed strep-MtrA was incubated with His-MtrR in concentrations ranging from 3 nM to 100 µM calculated based on the monomeric molecular mass. Based on two biological replicates the K_D was estimated to be 110 ± 30 nM.

MtrR modulates the Mtr-complex activity in vivo

A genetic approach was performed to allow insights into potential regulatory impacts of small protein MtrR on the Mtr-complex activity upon binding. The overproduction of MtrR-His$_6$ in *M. mazei* from a plasmid (pRS2087) does not affect the growth behavior under standard growth conditions with methanol as sole energy and carbon source. Further, a chromosomal deletion mutant of small ORF16 was constructed using an allelic replacement strategy through homologous recombination, replacing small ORF16 with a puromycin resistance cassette (*pac*) and verified by southern blot analysis

(supplemental Fig. S3). The growth behavior of this mutant strain (*M. mazei* Δ*sORF16*) under different growth conditions - varying the availability of carbon and energy sources as well as of molecular hydrogen (H_2) - was evaluated and compared to the wild type strain (Fig. 3). No effect was observed under standard growth conditions with methanol as the sole carbon and energy source with a gas phase consisting of N_2/CO_2 (v/v 80/20) (Fig. 3A). Under those conditions (methylotrophic methanogenesis), methanol is disproportionated, which means that 25% is oxidized to CO_2 and the electrons generated in this process are used to reduce 75% of the methanol to methane. When the N_2/CO_2 gas phase was changed to 100% H_2, the wild type grew faster and to a higher final cell density compared to growth under a N_2/CO_2 atmosphere (compare Fig. 3A and B, blue lines). This improved growth performance is based on the fact that under those growth conditions, molecular hydrogen is used as the electron donor, and consequently methanol is exclusively reduced to methane. In contrast, the *M. mazei* Δ*sORF16* mutant strain apparently does not benefit from the H_2 present in the gas phase, and shows the same growth behavior as in the absence of H_2, resulting in slower growth compared to the wild type and lower maximum cell density (Fig. 3B, orange line).

Further, when growing in the absence of methanol with CO_2 and H_2 as the main carbon and energy source in the gas phase (hydrogenotrophic methanogenesis), *M. mazei* Δ*sORF16* mutant strain again shows slower growth and reduced final cell density compared to the wild type (Fig. 3C, orange line). Together with the obtained biochemical data, these results strongly indicate a regulatory role of small protein MtrR in the energy metabolism at the methyl transfer step catalyzed by the Mtr complex, when H_2 is present as an electron donor.

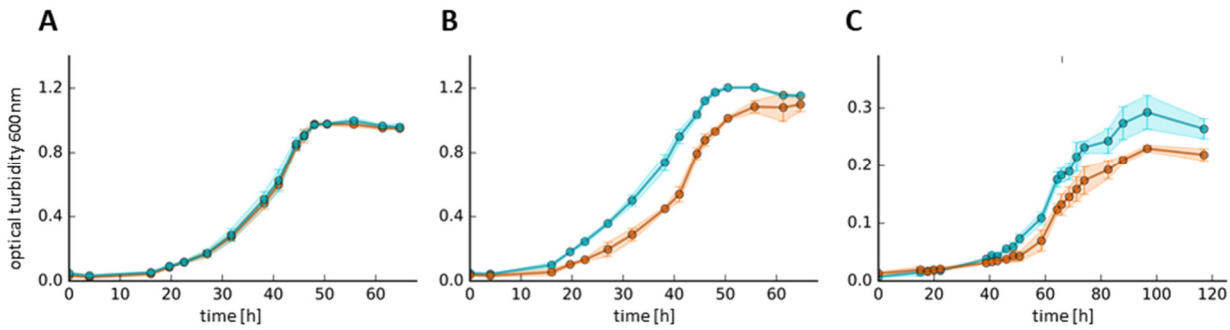

Fig. 3: Growth analysis of the *sORF16* deletion strain under different growth conditions. The growth behavior of *M. mazei* sORF16 chromosomal deletion mutant was studied under different growth conditions in comparison to the wt. 50 ml cultures were inoculated and incubated in closed 80 ml serum bottles under the respective gas phase. All growth curves represent the mean of three biological replicates each with several technical replicates, the standard deviation is indicated as error bars. *M. mazei* wt is generally depicted in blue and the deletion mutant ΔsORF16 in orange. **A:** Growth on 150 mM MeOH with a N_2/CO_2 (vol/vol, 80/20) gas phase. Inoculated from precultures grown on 150 mM MeOH with a N_2/CO_2 (vol/vol, 80/20) gas phase (methylotrophic growth). **B:** Growth on MeOH (150 mM) with a H_2 gas phase (100%). Inoculated from precultures grown on 150 mM MeOH

with a N_2/CO_2 (vol/vol, 80/20) gas phase. **C:** Growth on H_2/CO_2 (vol/vol, 80/20) as sole energy and carbon source in the gas phase (hydrogenotrophic). Inoculated from precultures grown without MeOH with a H_2/CO_2 (vol/vol, 80/20) gas phase. Please note the different scale of the y-axis in **C**.

Discussion

Aiming to functionally characterize the 49-aa small protein MtrR encoded by small ORF16, which was identified in *M. mazei* through ribosome profiling and mass spectroscopy (Tufail et al., 2024), we studied the small protein by biochemical and genetic approaches. We obtained strong experimental indications that the 5.5 kDa small protein is regulating the membrane-bound Mtr complex. We showed that MtrR, which lacks a membrane domain itself, is interacting with the membrane-bound Mtr complex resulting in the localization of oligomeric MtrR at the cytoplasmic membrane (Fig. 1C). In pull-down experiments using purified MtrR-His_6 and solubilized membranes, native MtrA and MtrH were copurified and identified by LC-MS/MS analysis (Fig. 2A). MtrR interaction with the Mtr complex was further confirmed by native and reversed copurification approaches (Fig. 2 BC) as well as by MST analysis between MtrR and MtrA showing high binding affinity (Fig. 2D).

The Mtr complex is one of the key enzymes of methanogenesis. It is a large, membrane-associated, multi-enzyme complex. In many methanogenic archaea, it facilitates the exergonic transfer of the methyl group from methyl tetrahydromethanopterin (CH_3-H_4MPT) to coenzyme M (HS-CoM) (ΔG = -30 kJ/mol) (Becher & Muller, 1994; Mand & Metcalf, 2019). In the case of *M. mazei*, the methyl group is bound to H_4SPT instead of H_4MPT, which is a derivative of methanopterin with a conjugated L-glutamic acid (Van Beelen et al., 1984). This Mtr reaction is coupled to sodium ion translocation over the cytoplasmic membrane, thereby contributing to energy conservation by establishing an ion gradient across the cytoplasmic membrane (Perski et al., 1982). Based on current molecular and structural studies, the large trimeric Mtr-complex consists of eight different subunits each, MtrABCDEFGH_2 (Aziz et al., 2024). MtrBCDEFG are transmembrane proteins with relatively small extracellular or cytoplasmic parts. MtrA consists of one transmembrane helix, which is bound to the membrane via the MtrBCDEFG complex, and another approximately 18-kDa soluble domain. MtrH is a soluble protein, but is associated as dimers with the membrane based on its interaction with MtrB and MtrF, which are part of the central transmembrane stalk (suppl. Fig. S4F). MtrH contains the binding site for CH_3-H_4SPT and transfers the methyl group onto a cobalamin bound by MtrA. After the methyl transfer, the methyl-cobalamin-carrying MtrA dissociates from MtrH and binds the MtrCDE subcomplex, which contains the cofactor HS-CoM, onto which the methyl group is transferred (suppl. Fig. S4F). In this manner, MtrA is predicted to perform a back-and-forth motion between MtrH and the membrane-bound MtrCDE (Aziz et al., 2024; Deppenmeier et al., 1996; Gottschalk & Thauer, 2001, Reiff-Trautmannsdorf et al. *in preparation*). Besides our finding of MtrR interacting with the Mtr-complex, there is further recent evidence that another small protein also binds to the Mtr complex (Reiff-Trautmannsdorf et al. *in preparation*).

The genus *Methanosarcina* shows the exceptional feature that the Mtr-complex can catalyze this methyl transfer in both directions depending on the environmental conditions, which enables methylotrophic, hydrogenotrophic or acetoclastic methanogenesis. When growing on methanol in the absence of H_2 as an electron donor, *M. mazei* needs to perform disproportionation of the methanol, where one mol of the methanol is oxidized to generate the electrons, which are required for the reduction of three other mol of methanol (Fig. 4C). The first step of the oxidative part is the transfer of the methyl group from CH_3-CoM to H_4SPT, performed by the Mtr-complex. Consequently, the Mtr reaction described above is reversed. Since the reversed reaction is thermodynamically unfavorable (ΔG = +30 kJ/mol), it is driven by the electrochemical membrane potential. Accordingly, it can be speculated that the direction of the Mtr reaction is strictly regulated depending on environmental conditions, such as available carbon sources and H_2 availability. However, a molecular mechanism of this potential regulation has not been described so far.

Our findings that MtrR interacts with the Mtr-complex in *M. mazei* and is conserved exclusively in the *Methanosarcina* genus, which is able to use diverse carbon and energy sources, hint towards a regulatory function of MtrR in the energy metabolism in response to changing conditions in carbon source and electron donors. MST experiments further showed that MtrR specifically binds the MtrA subunit. This observation is consistent with computational predictions obtained using AlphaFold3, which provide tentative structural insights into the potential interaction between MtrR and the Mtr (suppl. Fig. S4). MtrR (aa 24 - 28) might interact with the MtrA surface opposite of the cobalamin binding site containing the flexible loop of MtrA, which tethers the catalytic MtrA-domain to its membrane anchor (see suppl. Fig. S4). These interactions are presumably not hindering the transfer of the methyl group in general, but might impact MtrA to favor a transfer of the methyl group onto CoM instead of H_4SPT.

This hypothesis of MtrR favoring the methyl transfer from CH_3-H_4SPT to CoM is in agreement with obtained growth phenotypes of the chromosomal deletion mutant *(Δ*sORF16*) compared to the wild type under different growth conditions. *M. mazei* wild type, growing with methanol as carbon and energy source, performs better in presence of H_2, which serves as an electron donor to reduce the methanol to methane (Fig. 3). Consequently, the disproportionation of methanol (Fig. 4C) is no longer required and all methanol is reduced to methane (see Fig. 4B). The Δ*sORF16* mutant strain seems to fail to adapt to this condition which possibly results in continued partial oxidation of methanol, and consequently in less energy conservation and slower growth (Fig. 3B). In case of carbon dioxide and molecular hydrogen as the sole energy and carbon source (hydrogenotrophic methanogenesis), the Δ*sORF16* mutant strain also shows slower growth compared to the wild-type strain (Fig. 3C). This finding suggests that in the absence of MtrR, Mtr still partially catalyzes the transfer of the methyl

group from CoM to H_4SPT as part of the methyl-oxidizing pathway, resulting in lower energy yields and slower growth.

Overall, we conclude and propose that in the presence of H_2, the small protein MtrR plays an important role for the post-translational regulation of the key enzyme of methanogenesis, the membrane-bound Mtr complex, by favoring the methyl transfer from CH_3-H_4SPT to CoM (reducing direction), most likely by protein-protein interaction. This unique post-translational regulation of the Mtr complex by a small protein is beneficial for growth in the presence of H_2 with either methanol or carbon dioxide as a carbon source (Fig. 4). Moreover, the findings argue for a direct link between small protein modulation, energy conservation, and environmental sensing in methanoarchaea. It is further attractive to speculate that, based on the H_2 presence or the energy demand of the cell, MtrR is upregulated or activated and subsequently regulates the Mtr complex by binding to MtrA. Future investigations of this regulation by MtrR on the molecular and structural level as well as addressing the signaling pathway of H_2 availability will reinforce our understanding of the detailed regulation of the Mtr activity .

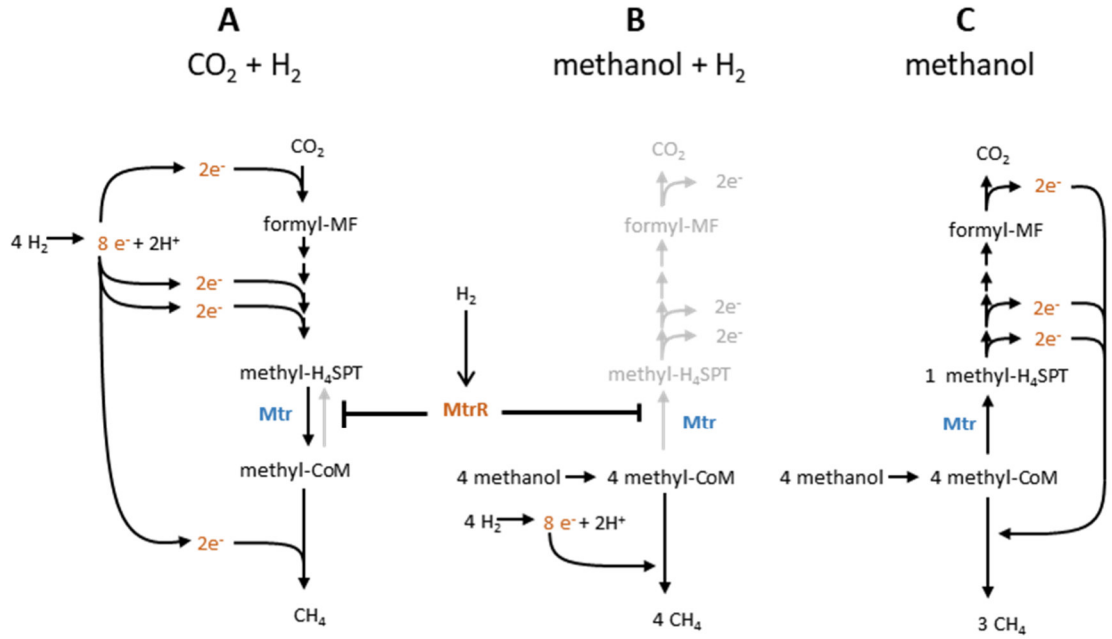

Fig. 4: Hypothetical model of Mtr regulation by MtrR. Simplified schematic cartoons of methanogenesis in *M. mazei* under three different conditions: **A**: CO_2 as sole carbon and energy source in combination with molecular hydrogen (H_2). **B/C**: Growth on methanol with H_2 (**B**) and without H_2 (**C**) in the gas phase. We propose that MtrR in the presence of H_2 is required for favoring the methyl transfer from CH_3-H_4SPT to CoM (reducing direction) most likely by protein-protein interaction.

Methods

Protein structure prediction

Protein structure prediction was conducted using AlphaFold3 via the AlphaFold3 Server (Abramson et al., 2024; Jumper et al., 2021).

Construction of strains and plasmids

Small ORF16 genomic deletion

The 1-kb genomic regions flanking the small ORF16 gene on both sides were amplified from *M. mazei* Gö1 genomic DNA using specific primers (Eurofins, Ebersberg, Germany) listed in Table S2. A puromycin resistance (PurR) cassette (Metcalf et al., 1997), encoding the puromycin *N*-acetyltransferase gene from *Streptomyces alboniger* combined with a *M. mazei* constitutive promotor pmcrB, was cut from pRS207 (Table S1) using *Bam*HI. The 1-kb upstream and downstream fragments were inserted in the plasmid pMCL210 using restriction enzymes *Kpn*I and *Not*I. The plasmid pMCL210

(Nakano et al., 1995) was used as a suicide vector for allelic replacement in *M. mazei* (Hüttermann & Schmitz, 2024). The resulting plasmid was designated pRS2037. pRS2037 was linearized using *Sal*I and subsequently transformed into *M. mazei* using liposome-mediated transformation (Ehlers et al., 2005). The small ORF16 gene was replaced by the *pac*-cassette using the 1kb flanking regions for double homologous recombination. Successfully recombined cells with the small ORF16 deletion were selected in puromycin-containing medium, and later plated to obtain single mutant clones (Uwe Deppenmeier et al., 2002). The success of the deletion was further analyzed via southern blotting using specific probes against the small ORF16 gene and the *pac* cassette (Fig S3).

Small ORF16 expression mutant

The gene encoding MtrR was amplified from *M. mazei* genomic DNA using specific primers (Eurofins, Ebersberg, Germany; listed in Table S2), and used for restriction ligation cloning in pET21a using *Nde*I and *Not*I restriction enzymes (New England Biolabs, Ipswich, USA) and T4 ligase (Thermo Fisher Scientific, Waltham, MA, USA). The resulting plasmid was named pRS1834. The plasmid pRS1834 was transformed into competent (Inoue et al., 1990) *E. coli* BL21 pRIL (Table S1) for heterologous expression. The small ORF16-His_6 fusion was further amplified from pRS1834 and cloned into pRS1807 behind an *M. mazei* constitutive promotor pmcrB using restriction enzymes *Bam*HI and *Not*I (New England Biolabs, Ipswich, USA) and T4 ligase (Thermo Fisher Scientific, Waltham, MA, USA). The obtained plasmid was named pRS2087, which was transformed into *M. mazei* using liposome-mediated transformation (Ehlers et al., 2005).

The nucleotide sequence of the soluble part (aa 1-168) of the *mtrA* gene without the transmembrane domain (aa 169-240) was amplified from *M. mazei* genomic DNA using specific primers (Eurofins, Ebersberg, Germany; listed in Table S2), and used for cloning in pRS1736 using B*sa*I restriction enzyme (New England Biolabs, Ipswich, USA) and T4 ligase (Thermo Fisher Scientific, Waltham, MA, USA). The resulting plasmid was named pRS2190. The plasmid pRS2190 was transformed into competent (Inoue et al., 1990) *E. coli* BL21 pRIL (Table S1) for heterologous expression.

Purification heterologously expressed proteins

E. coli BL21 (DE3)/pRIL cultures containing the respective expression plasmid were grown in Terrific Broth (TB) medium under continuous shaking at 37 °C. At optical turbidity of T600 = 0.8, protein expression was induced by adding IPTG to a final concentration of 100 µM. After additional incubation for 2 hours, cells were harvested by centrifugation at 4,000 x g at 4 °C for 20 min. The cells were resuspended in 6 mL phosphate buffer A (50 mM sodium phosphate, 300 mM NaCl, pH 8.0) and lysed by passing the French pressure cell two times with 80 N/mm^2. To get rid of unlysed cells and cell debris, the cell extract was centrifuged again for another 30 min at 13,000xg at 4°C. His tagged

proteins were purified using IMAC using Ni-NTA on gravity columns with 1 ml bed volume. The elution was conducted using phosphate buffer (50 mM sodium phosphate, 300 mM NaCl, pH 8.0) with imidazole in steps with 100 mM, 250 mM and 500 mM in phosphate buffer A. Strep-tagged proteins were purified with strep tactin sepharose (IBA Lifesciences, Göttingen, Germany) and eluted with 2.5 mM desthiobiotin in Tris/HCl buffer (100 mM Tris-HCl, 150 mM NaCl, 2.5 mM EDTA pH 8.0). Subsequently, the buffer was exchanged to phosphate buffer (50 mM sodium phosphate, 300 mM NaCl, pH 8.0).

If needed, further purification was done via size exclusion chromatography (SEC) using a gel filtration column Enrich TM SEC 650 (BioRad, Hercules, USA). The protein was eluted with a flow rate of 1 ml/min in phosphate buffer (50 mM sodium phosphate, 300 mM NaCl, pH 8.0).

MtrR-His_6 purified to homogeneity (Fig. 1B, 13 ml) was used to generate polyclonal antibodies by Davids Biotechnologie (Regensburg, Deutschland).

Growth of *M. mazei* and subcellular fractionation

Under standard conditions, *M. mazei* was cultivated in 1 L anaerobic minimal medium in 2 L sealed bottles or in 50 mL anaerobic minimal medium (U. Deppenmeier et al., 1990) in 80 mL serum bottles with a gas phase consisting of N_2 and CO_2 in an 80/20 (vol/vol,) ratio (2 bar). Right before inoculation, the medium was complemented with 150 mM methanol as the carbon source. For growth phenotype experiments, the gas phase was changed to H_2/CO_2 in an 80/20 (vol/vol) ratio or 100% H_2 (2 bar) with or without methanol.

M. mazei cells were harvested by centrifugation at 6,000 x g at 4 °C for 45 min. Cells were lysed using a dismembrator (Sartorius, Göttingen, Germany) at 1,600 rpm for 3 min in Tris buffer (50mM, pH 7.6).

Subcellular fractionation was done by centrifugation at 200,000 x g at 4 °C for 1 h. The supernatant was labeled as cytoplasmic fraction. The obtained pellet was washed in Tris buffer and centrifuged again in the same manner, and the resulting pellet was labelled as membrane fraction. The resulting membrane pellet was solubilized by adding a final concentration of either 2% DDM or 1% LMNG and gentle shaking for 1 h at 4 °C and subsequently centrifuged again at 210,000 x g and 4 °C for 1 h.

When subcellular fractions were analyzed on SDS PAGE, samples were not heated prior to loading to prevent aggregation of membrane proteins.

Pull-down from *M. mazei* and LC-MS/MS analysis

Heterologously expressed, purified MtrR-His_6 was used as the bait protein for in vitro pull-downs of potentially interacting proteins from solubilized membrane fractions. For that, His_6-MtrR was purified using IMAC and subsequent SEC to obtain protein fractions of high purity (see Fig. 1B) as bait for pull-down experiments. Membrane fractions of *M. mazei* were prepared by subcellular fractionation from exponentially growing cells at optical turbidity of 0.6 as described above. The resulting membrane fraction (total protein content of 5 mg) was incubated with bait protein (0.5 mg purified MtrR-His_6) followed by IMAC purification of MtrR-His_6 using 0.1 ml Ni-NTA agarose resin (Qiagen, Hilden, Germany). As negative controls, the membrane fraction (total protein content of 5 mg) without the bait MtrR-His_6 was treated in the same manner. Potential interaction partners for the small protein MtrR were identified from the elution via GeLC-MS. Briefly, triplicate samples and the respective controls were separated across 12% SDS-PAGE and stained with Coomassie brilliant blue. Before the loading on SDS gels, samples of membrane proteins were not heated in order to prevent aggregation of the membrane proteins.

Protein bands present in the sample but not in the control gels were excised, with comparable regions from the control gels also processed. The excised areas were cut into cubes *ca.* 1mm^3, and de-stained with successive washes of acetonitrile and 100mM ammonium bicarbonate buffer, pH 7.4. In gel reduction (10 mM dithiothreitol, 56°C, 1 hr), and alkylation (50 mM chloroacetamide, 20°C, 30 min), of the samples was performed, followed by overnight enzymatic digestion with sequencing-grade trypsin (20 ng/band, in 100 mM ammonium bicarbonate buffer, pH 7.4, 37°C). Following digestion, the peptides in the aqueous solution were collected, with two subsequent extractions of the hydrophobic peptides with 60% acetonitrile + 0.1% trifluoroacetic acid and then 100% acetonitrile. Both extractions were pooled with the aqueous solution for the corresponding sample, before being dried via vacuum centrifugation.

The peptides were re-suspended in 3% acetonitrile +0.05% trifluoroacetic acid immediately before LC-MS analysis.

One-dimensional liquid chromatography separation of the peptides was performed on a Dionex U3000RSLC nanoHPLC (Thermo Fisher Scientific, Germany) across an acclaimpepmap100 C18 column (2µm particle size, id75 µm x 500 mm) coupled online to a Q Exactive Plus mass spectrometer (Thermo Fisher Scientific, Germany). Eluent A:0.05% formic acid, Eluent B:80% acetonitrile+0.04% formic acid. The separation was performed over a programmed 60 min run. Initial chromatographic conditions were 4% B for 3 min followed by linear gradients from 4% to 50% B over 30 min, then 50 to 90% over 1 min, and 10 min at 90% B. Following this, an inter-run equilibration of the column was achieved by 15 minutes at 4% B. A 300 nl/min flow rate and 5 µl were injected per run.

Data acquisition on a Q Exactive plus mass spectrometer was performed using data-dependent acquisition with full scan MS acquisition (300-1500 m/z, resolution 70,000) and subsequent MS/MS of the top 10 most intense ions via HCD activation at NCE 27 (resolution 17,500); dynamic exclusion was enabled (20 sec duration).

Data analysis was performed using Proteome Discoverer (Ver 3.1.1.93) and the SequestHT search algorithm. MS raw files were searched against the *M. mazei* Gö1 database including all predicted SEP protein sequences (accession date 2024.06.19), and the cRAP list of common laboratory contaminants. Searches were performed with trypsin specificity and a maximum of 2 missed cleavages, methionine oxidation was set as a variable modification, and cysteine carbamidomethylation was set as a fixed modification. The raw data files can be found in the ProteomeXchange repository (identifier PSD064332 (Röst et al., 2014).

Microscale thermophoresis

Proteins were purified to apparent homogeneity by affinity chromatography using Ni-NTA agarose (Qiagen, Hilden, Germany) and labeled with the RED-NHS, 2nd generation, 650 nm fluorescent dye using the Monolith NT RED-NHS lysine labeling kit according to the manufacturer's protocol (NanoTemper, Munich, Germany). RED-labeled strep-tagged MtrA at 20 nM and MtrR-His$_6$ in 16 different concentrations ranging from 100 µM to 3 nM (concentrations based on monomeric molecular mass) was used. The protein interaction was measured in standard capillaries (Nanotemper, Munich, Germany), 100% excitation power and medium MST power (IR-laser intensity). The interaction was tested in two biological replicates. MST traces were analyzed in MO. Affinity Analysis (Nanotemper, Munich, Germany).

Acknowledgements

We thank the groups of AG Schmitz-Streit and AG Schuller for fruitful discussions and critical comments on the project. This work was supported by the German Research Foundation (DFG) priority program SPP2002 "Small Proteins in Prokaryotes, an Unexplored World" RSCHM1052/20-1 and 20-2, RSCHM1052/19-2 to RAS; TH872/10-1 and 10-2 to A.T. J.M.S. acknowledges the DFG for an Emmy Noether grant (SCHU 3364/1-1), RTG 2937 and the European Union's Horizon 2020 research and innovation programme (Two-CO2-One; grant agreement no. 101075992). The views and opinions expressed are those of the author(s) only and do not necessarily reflect those of the European Union

or the European Research Council. Neither the European Union nor the granting authority can be held responsible for them.

Conflict of interest

The authors declare that they have no conflict of interest.

Author contribution

RAS initiated the project. TH and RAS designed the experiments. TH performed the majority of the experiments. BH and CK contributed to cloning of expression mutants and *in vivo* interaction experiments. LC and AT performed the LC-MS/MS analysis of MtrR interacting proteins. TH wrote the manuscript together with RAS. TH, RAS and JMS interpreted the results and finalized the results. RAS supervised the research and provided resources and funding. All authors approved the submitted version.

References

Abramson, J., Adler, J., Dunger, J., Evans, R., Green, T., Pritzel, A., Ronneberger, O., Willmore, L., Ballard, A. J., Bambrick, J., Bodenstein, S. W., Evans, D. A., Hung, C. C., O'Neill, M., Reiman, D., Tunyasuvunakool, K., Wu, Z., Žemgulytė, A., Arvaniti, E., … Jumper, J. M. (2024). Accurate structure prediction of biomolecular interactions with AlphaFold 3. *Nature*, *630*(8016), 493–500. https://doi.org/10.1038/s41586-024-07487-w

Aziz, I., Kayastha, K., Kaltwasser, S., Vonck, J., Welsch, S., Murphy, B. J., Kahnt, J., Wu, D., Wagner, T., Shima, S., & Ermler, U. (2024). Structural and mechanistic basis of the central energy-converting methyltransferase complex of methanogenesis. *Proceedings of the National Academy of Sciences of the United States of America*, *121*(14), 2315568121. https://doi.org/10.1073/PNAS.2315568121/FORMAT/EPUB

Becher, B., & Muller, V. (1994). Δμ(Na+) drives the synthesis of ATP via an Δμ(Na+)-translocating F1F0-ATP synthase in membrane vesicles of the archaeon Methanosarcina mazei Go1. *Journal of Bacteriology*, *176*(9), 2543–2550. https://doi.org/10.1128/jb.176.9.2543-2550.1994

Cassidy, L., Kaulich, P. T., Maaß, S., Bartel, J., Becher, D., & Tholey, A. (2021). Bottom-up and top-down proteomic approaches for the identification, characterization, and quantification of the low molecular weight proteome with focus on short open reading frame-encoded peptides. *Proteomics*, *21*. https://doi.org/10.1002/pmic.202100008

Costa, K. C., & Leigh, J. A. (2014). Metabolic versatility in methanogens. *Current Opinion in Biotechnology*, *29*(1), 70–75. https://doi.org/10.1016/j.copbio.2014.02.012

Deppenmeier, U., Blaut, M., Mahlmann, A., & Gottschalk, G. (1990). Reduced coenzyme F420: Heterodisulfide oxidoreductase, a proton-translocating redox system in methanogenic bacteria. *Proceedings of the National Academy of Sciences of the United States of America*, *87*(23), 9449–9453. https://doi.org/10.1073/pnas.87.23.9449

Deppenmeier, Uwe, Johann, A., Hartsch, T., Merkl, R., Schmitz, R. A., Martinez-Arias, R., Henne, A., Wiezer, A., Bäumer, S., Jacobi, C., Brüggemann, H., Lienard, T., Christmann, A., Bömeke, M., Steckel, S., Bhattacharyya, A., Lykidis, A., Overbeek, R., Klenk, H. P., … Gottschalk, G. (2002). The genome of Methanosarcina mazei: Evidence for lateral gene transfer between bacteria and archaea. *Journal of Molecular Microbiology and Biotechnology*, *4*(4), 453–461.

Deppenmeier, Uwe, Müller, V., & Gottschalk, G. (1996). Pathways of energy conservation in methanogenic archaea. *Archives of Microbiology*, *165*(3), 149–163. https://doi.org/10.1007/BF01692856

Ehlers, C., Weidenbach, K., Veit, K., Deppenmeier, U., Metcalf, W. W., & Schmitz, R. A. (2005). Development of genetic methods and construction of a chromosomal glnK 1 mutant in Methanosarcina mazei strain Gö1. *Molecular Genetics and Genomics*, *273*(4), 290–298. https://doi.org/10.1007/s00438-005-1128-7

Gelsinger, D. R., Dallon, E., Reddy, R., Mohammad, F., Buskirk, A. R., & DiRuggiero, J. (2021). Ribosome profiling in archaea reveals leaderless translation, novel translational initiation sites, and ribosome pausing at single codon resolution. *Nucleic Acids Research*, *48*(10), 5201–5216. https://doi.org/10.1093/NAR/GKAA304

Gottschalk, G., & Thauer, R. K. (2001). The Na+-translocating methyltransferase complex from methanogenic archaea. In *Biochimica et Biophysica Acta - Bioenergetics* (Vol. 1505, Issue 1, pp. 28–36). https://doi.org/10.1016/S0005-2728(00)00274-7

Grahame, D. A. (1991). Catalysis of acetyl-CoA cleavage and tetrahydrosarcinapterin methylation by a carbon monoxide dehydrogenase-corrinoid enzyme complex. *Journal of Biological Chemistry*, *266*(33), 22227–22233. https://doi.org/10.1016/S0021-9258(18)54558-0

Gray, T., Storz, G., & Papenfort, K. (2022). Small Proteins; Big Questions. *Journal of Bacteriology*, *204*(1). https://doi.org/10.1128/JB.00341-21

Gutt, M., Jordan, B., Weidenbach, K., Gudzuhn, M., Kiessling, C., Cassidy, L., Helbig, A., Tholey, A., Joshua Pyper, D., Kubatova, N., Schwalbe, H., Anne Schmitz, R., & Schmitz, R. A. (2021). High complexity of Glutamine synthetase regulation in Methanosarcina mazei: Small protein 26 interacts and enhances glutamine synthetase activity. *The FEBS Journal*. https://doi.org/10.1111/febs.15799

Habenicht, T., Weidenbach, K., Velazquez-Campoy, A., Buey, R. M., Balsera, M., & Schmitz, R. A. (2023). Small protein mediates inhibition of ammonium transport in Methanosarcina mazei —an ancient mechanism? . *Microbiology Spectrum*, *11*(6). https://doi.org/10.1128/SPECTRUM.02811-23/SUPPL_FILE/SPECTRUM.02811-23-S0005.DOCX

Hadjeras, L., Bartel, J., Maier, L.-K. K., Maaß, S., Vogel, V., Svensson, S. L., Eggenhofer, F., Gelhausen, R., Müller, T., Alkhnbashi, O. S., Backofen, R., Becher, D., Sharma, C. M., & Marchfelder, A. (2023). Revealing the small proteome of Haloferax volcanii by combining ribosome profiling and small-protein optimized mass spectrometry. *MicroLife*, *4*, 1–17. https://doi.org/10.1093/femsml/uqad001

Hanahan, D. (1983). Studies on transformation of Escherichia coli with plasmids. *Journal of Molecular Biology*, *166*(4), 557–580. https://doi.org/10.1016/S0022-2836(83)80284-8

Hedderich, R., Hamann, N., & Bennati, M. (2005). Heterodisulfide reductase from methanogenic archaea: A new catalytic role for iron-sulfur cluster. *Biological Chemistry*, *386*(10), 961–970. https://doi.org/10.1515/BC.2005.112

Hippe, H., Casparit, D., Fiebigt, K., & Gottschalkt, G. (1979). *Utilization of trimethylamine and other N-methyl compounds for growth and methane formation by Methanosarcina barkeri* (Vol. 76, Issue 1).

Huang, G., Wagner, T., Ermler, U., & Shima, S. (2020). Methanogenesis involves direct hydride transfer from H2 to an organic substrate. *Nature Reviews Chemistry*, *4*(4), 213–221. https://doi.org/10.1038/s41570-020-0167-2

Hüttermann, J., & Schmitz, R. (2024). Compiling a versatile toolbox for inducible gene expression in Methanosarcina mazei. *MicroLife*, *5*. https://doi.org/10.1093/femsml/uqae019

Inoue, H., Nojima, H., & Okayama, H. (1990). High efficiency transformation of Escherichia coli with plasmids. *Gene*, *96*(1), 23–28. https://doi.org/10.1016/0378-1119(90)90336-P

Jaun, B., & Thauer, R. K. (2007). Methyl-Coenzyme M Reductase and its Nickel Corphin Coenzyme F430 in Methanogenic Archaea. In *Nickel and Its Surprising Impact in Nature* (Vol. 2). https://doi.org/10.1002/9780470028131.ch8

Jordan, B., Weidenbach, K., & Schmitz, R. A. (2023). The power of the small: the underestimated role of small proteins in bacterial and archaeal physiology. *Current Opinion in Microbiology*, *76*, 102384. https://doi.org/10.1016/J.MIB.2023.102384

Jumper, J., Evans, R., Pritzel, A., Green, T., Figurnov, M., Ronneberger, O., Tunyasuvunakool, K., Bates, R., Žídek, A., Potapenko, A., Bridgland, A., Meyer, C., Kohl, S. A. A., Ballard, A. J., Cowie, A., Romera-Paredes, B., Nikolov, S., Jain, R., Adler, J., … Hassabis, D. ✉. (2021). Highly accurate protein structure prediction with AlphaFold. *Nature*, *596*, 583. https://doi.org/10.1038/s41586-021-03819-2

Li, L., Li, Q., Rohlin, L., Kim, U. M., Salmon, K., Rejtar, T., Gunsalus, R. P., Karger, B. L., & Ferry, J. G. (2007). Quantitative Proteomic and Microarray Analysis of the Archaeon Methanosarcina acetivorans Grown with Acetate versus Methanol. *Journal of Proteome Research*, *6*(2), 759–771. https://doi.org/10.1021/pr060383l

Liu, Y., & Whitman, W. B. (2008). Metabolic, phylogenetic, and ecological diversity of the methanogenic archaea. *Annals of the New York Academy of Sciences*, *1125*, 171–189. https://doi.org/10.1196/annals.1419.019

Mand, T. D., & Metcalf, W. W. (2019). Energy Conservation and Hydrogenase Function in Methanogenic Archaea, in Particular the Genus Methanosarcina . *Microbiology and Molecular Biology Reviews*, *83*(4). https://doi.org/10.1128/MMBR.00020-19/ASSET/A6A53F58-6481-4E93-B801-961F2ADE3A2F/ASSETS/GRAPHIC/MMBR.00020-19-F0010.JPEG

Metcalf, W. W., Zhang, J. K., Apolinario, E., Sowers, K. R., & Wolfe, R. S. (1997). A genetic system for Archaea of the genus Methanosarcina: Liposome-mediated transformation and construction of shuttle vectors. *Proceedings of the National Academy of Sciences of the United States of America*, *94*(6), 2626–2631. https://doi.org/10.1073/pnas.94.6.2626

Miroux, B., & Walker, J. E. (1996). Over-production of Proteins in Escherichia coli: Mutant Hosts that Allow Synthesis of some Membrane Proteins and Globular Proteins at High Levels. In *J. Mol. Biol* (Vol. 260).

Nakano, Y., Yoshida, Y., Yamashita, Y., & Koga, T. (1995). Construction of a series of pACYC-derived plasmid vectors. *Gene*, *162*(1), 157–158. https://doi.org/10.1016/0378-1119(95)00320-6

Perski, H. J., Schönheit, P., & Thauer, R. K. (1982). Sodium dependence of methane formation in methanogenic bacteria. *FEBS Letters*, *143*(2), 323–326. https://doi.org/10.1016/0014-5793(82)80126-9

Prasse, D., Thomsen, J., De Santis, R., Muntel, J., Becher, D., & Schmitz, R. A. (2015). First description of small proteins encoded by spRNAs in Methanosarcina mazei strain Gö1. *Biochimie*, *117*, 138–148. https://doi.org/10.1016/j.biochi.2015.04.007

Röst, H. L., Rosenberger, G., Navarro, P., Gillet, L., Miladinović, S. M., Schubert, O. T., Wolski, W., Collins, B. C., Malmström, J., Malmström, L., & Aebersold, R. (2014). ProteomeXchange provides globally coordinated proteomics data submission and dissemination. *26. Deutsch, E.W. Mol. Cell. Proteomics*, *32*(23), 1683–1695. https://doi.org/10.1038/nbt.2841

Storz, G., Wolf, Y. I., & Ramamurthi, K. S. (2014). Small Proteins Can No Longer Be Ignored. *Annual Review of Biochemistry*, *83*(1), 753–777. https://doi.org/10.1146/annurev-biochem-070611-102400

Tufail, M. A., Jordan, B., Hadjeras, L., Gelhausen, R., Cassidy, L., Habenicht, T., Gutt, M., Hellwig, L., Backofen, R., Tholey, A., Sharma, C. M., & Schmitz, R. A. (2024). Uncovering the small proteome of Methanosarcina mazei using Ribo-seq and peptidomics under different nitrogen conditions. *Nature Comm*. https://doi.org/10.1038/s41467-024-53008-8

Üresin, D., Pyper, D. J., Borst, A., Hadjeras, L., Gelhausen, R., Backofen, R., Sharma, C., Schwalbe, H., & Soppa, J. (2023). Characterization of the zinc finger µ-protein HVO_0758 from Haloferax volcanii:

biological roles, zinc binding, and NMR solution structure. *Frontiers in Microbiology*, *14*. https://doi.org/10.3389/FMICB.2023.1280972/FULL

Van Beelen, P., Labro, J. F. A., Keltjens, J. T., Geerts, W. J., Vogels, G. D., Laarhoven, W. H., Guijt, W., & Haasnoot, C. A. G. (1984). Derivatives of methanopterin, a coenzyme involved in methanogenesis. *Eur. J. Biochem*, *139*, 359–365. https://doi.org/10.1111/j.1432-1033.1984.tb08014.x

Weidenbach, K., Gutt, M., Cassidy, L., Chibani, C., & Schmitz, R. A. (2021). Small proteins in Archaea, a mainly unexplored world. *Journal of Bacteriology*. https://doi.org/10.1128/JB.00313-21

Yi, Y., Dolfing, J., Jin, G., Fang, X. Y., Han, W. H., Liu, L. Y., Tang, Y. Q., & Cheng, L. (2023). Thermodynamic restrictions determine ammonia tolerance of methanogenic pathways in Methanosarcina barkeri. *Water Research*, *232*, 119664. https://doi.org/10.1016/J.WATRES.2023.119664

Zahn, S., Kubatova, N., Pyper, D. J., Cassidy, L., Saxena, K., Tholey, A., Schwalbe, H., Org Soppa, J. ¨, & Schwalbe, H. (2021). Biological functions, genetic and biochemical characterization, and NMR structure determination of the small zinc finger protein HVO_2753 from Haloferax volcanii. *The FEBS Journal*, *288*, 2042. https://doi.org/10.1111/febs.15559